JOURNAL OF MATERIALS SCIENCE 28 (1993) 2385–2390

Mechanical properties of hot isostatically pressed zirconium nitride materials

N. ALEXANDRE, M. DESMAISON-BRUT
Laboratoire de Céramiques Nouvelles, URA CNRS 320, 123, Avenue Albert Thomas, 87060 Limoges Cedex, France

F. VALIN, M. BONCOEUR
CEN–Saclay, 91191 Gif-sur-Yvette Cedex, France

The influence of powder properties on the sintering behaviour, the microstructural development and the mechanical properties of hot isostatically pressed (HIPed) zirconium nitrides were investigated. The results show that the densification behaviour is dependent on the powder characteristics, more precisely the grain morphology and size, and oxygen, carbon and metallic impurity contents. The mechanical properties are controlled mainly by the amount of porosity and the presence of a complex intergranular phase in direct relation to the purity of the starting powder. The differences in the fracture strength and toughness between the two grades are perceptible. On the other hand, the thermal shock resistance to fracture initiation, as well as the elastic parameters of both dense materials, are similar.

1. Introduction

Obtaining full densification without a consolidation additive has attracted the attention of researchers. This goal may be reached by HIPing. Therefore, the aim of this work was to elaborate fully dense zirconium nitride materials by applying this technique.

Zirconium nitride, as well as several other types of transition-metal nitrides (tantalum, hafnium and titanium nitrides) has a high melting point. Industrial uses as refractories have been limited by their poor oxidation resistance. On the other hand, ZrN is resistant to the attack of molten metals such as Ce, Fe and Be. Therefore, the properties of ZrN crucibles, formed by pressing in steel dies, have been studied extensively [1]. ZrN crucibles were prepared from finely divided powder, fired at high temperature to produce a material with zero porosity. Their surfaces were very hard, but could be scratched by tungsten carbide or diamond and be induction-heated to 2200 °C and cooled rapidly without cracking.

Petrykina and Shvedova [2] showed that the sintering of transition-metal nitride powders by the hot-pressing technique enables dense nitride parts to be produced. The sintering experimental conditions of 2500 °C at 45 MPa for 5 min yield a material of 99% relative density which is slightly substoichiometric (ZrN_x, $x = 0.95$).

The sintering of zirconium nitride in vacuum and in nitrogen was investigated by Pshenichnaya *et al.* [3]. By using fine powders of < 1 μm particle size, treated in vacuum at 2100 °C, parts with relative densities of 95% were produced. However, under these conditions the composition of nitride shifts towards the lower limit of its homogeneity range. To retain the approximately stoichiometric composition, it is necessary either to perform sintering in a nitrogen atmosphere at temperatures above 2000 °C or to subject vacuum-sintered blanks to prolonged additional annealing in nitrogen. Moreover, well-adherent zirconium nitride coatings have been produced using the arc vapour ion deposition process [4].

In order to define more precisely the sintering conditions leading to the elaboration of dense materials, we analysed the HIPing behaviour of two commercially available zirconium nitride powders. The influence of the working parameters (temperature and dwell time) on the densification is discussed, and relationships between the mechanical properties and the microstructures are established.

2. Materials and methods

2.1. Characteristics of powders

The first commercial grade powder was supplied by Cerac (USA). Its particle size distribution, determined by sedigraphy, varied from 1 to 50 μm (Fig. 1). A significant amount of the powder consisted of large irregular grains. The average particle size was 9.35 μm and the specific surface area was 0.373 $m^2 g^{-1}$. This material contained 2.4 % hafnium.

The second grade was supplied by H. C. Starck. The grain shape was less irregular. A maximum particle size of 4.4 μm and a specific surface area of 0.752 $m^2 g^{-1}$ were determined (Fig. 1).

The main characteristics of the starting powders are listed in Table I. X-ray diffraction analysis indicated

0022–2461

TABLE I Chemical analysis of starting powders (wt %)

	N	Hf	O	C	Al	Si	Ti	Fe	Cr	Mg
Cerac	11.2	2.4	2.1	0.5	0.04	0.01	0.03	0.04	0.02	0.001
Starck	12.4	0.2	0.92	0.15	0.02	0.02	0.01	0.2	0.03	0.02

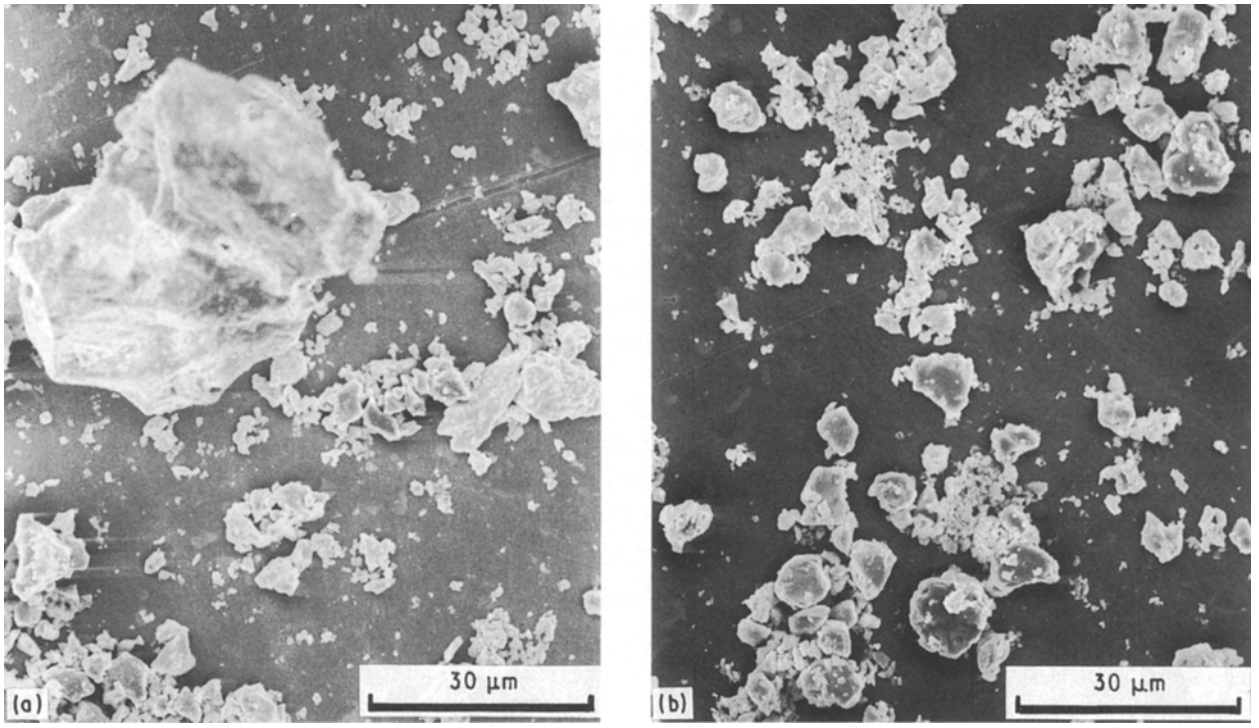

Figure 1 SEM micrographs of the ZrN powders: (a) Cerac and (b) Starck.

that the powders were stoichiometric (lattice parameters 0.457 70 and 0.457 60 nm).

2.2. Process

The powders were sieved at 40 μm. Approximately 250 g zirconium nitride was cold isostatically pressed at 250 MPa pressure. The green density was close to 65% theoretical. The green moulded material was introduced either into a silica container or into a titanium container. An inert layer, which acted as a diffusion barrier, was necessary to prevent chemical reactions between the capsule and the component. Degassing was carried out at 600 °C in vacuum (10^{-4} Pa) for 12 h. The HIP parameters (temperature and pressure) were defined by taking into consideration the plastic deformation of the container. Then the ceramic material was sintered by HIPing either at 1600 °C (titanium container) or at 1950 °C (SiO_2 capsule). The maximum pressure, applied in an Alsthom press, was 195 MPa. The dwell time was 1 or 2 h. Mechanical decapsulation was performed without any parts being damaged.

2.3. Specimen characterization

Zirconium nitride density measurements were done using the Archimedes method. The microstructure was controlled by scanning electron microscopy (SEM) observations on chemically etched samples (etching medium HF/HNO_3). Microhardness tests (Shimadzu apparatus) were carried out using a selected load of 0.2 kg.

The conventional single edge notched beam (SENB) method was used to determine the critical stress intensity (K_{Ic}) factor on a minimum of four samples. In choosing this K_{Ic} measurement technique we were influenced by the precision of the test method and its reproducibility. Special attention has already been devoted to the influence of the notch width on the measured value of K_{Ic} [5]. Profile control was done by image analysis and confirmed the reproducibility of the curvature radius, equal to 60 μm at the bottom of the notch.

Three-point bending strength measurements were carried out with a Wolpert machine (load application speed 0.2 mm min^{-1}, span distance 19 mm and with seven 4 mm × 4 mm × 22 mm bars tested).

Thermal quenching was performed by heating the specimen (4 mm × 4 mm × 22 mm bar) in a furnace and then dropping it into a room-temperature water bath. Fracture strength comparisons were made by breaking the bars after water shocking.

The Young's modulus and Poisson's ratio were determined at room temperature by the disc vibration technique. The shear modulus was calculated from these two constants.

3. Results and discussion

3.1. Characterization of the final product

Under the best conditions and independently of the initial powder used, more than 99% theoretical density was achieved. The HIPing of the Cerac powder was studied first. A series of experiments was performed in titanium containers at 1600 °C with an up-holding dwell time of 1 h. The pressure conditions varied from 120 to 190 MPa. The relative densities ranged, respectively, from 91.7 to 95.5%.

By using a silica capsule, at temperatures varying from 1600 to 1950 °C, under a constant pressure of 190 MPa, an increase in relative density was observed from 95.5 to 97.1%. It is also noted that increasing the dwell time increased the shrinkage. The best material (relative density > 99%) was obtained by HIPing the powder for 2 h at 1950 °C and 195 MPa.

Secondly, HIPing was applied to the powder supplied by H.C. Starck. This powder was densified in a titanium container at 1600 °C, for 1 or 2 h, at a pressure of 195 MPa. In this case also, a relative density of > 99% was reached.

3.2. Morphological observations

Microscopic observations of the first grade showed the presence of two phases, one of which seemed to be preferentially located along the grain boundaries. The pore shape and the localization of the secondary phase depended on the experimental conditions. When the pressure increased, the pores became spherical and the secondary phase was progressively forced back towards the triple points. This phase was similar to the liquid phase formed by classical sintering with additives (Fig. 2a and e). Otherwise, in the temperature range 1500–1650 °C, there was no change in the quantity of intergranular phase.

Electron-probe microanalysis (EPMA) of this secondary phase showed that not only were the impurities segregated into the grain-boundary phase, but also the oxygen concentration was higher whereas the nitrogen concentration was lower. Some authors have reported the possible formation of various phases such as Zr_2ON_2, $Zr_7O_8N_4$ and $Zr_7O_{11}N_2$ [6, 7].

For the second grade the presence, on SEM micrographs, of an oxynitride phase located between the grains was not so evident. This is in agreement with the lower content of oxygen, carbon and impurities in the starting powder. Small spheres are regularly distributed between zirconium nitride grains (Fig. 2b). The globulization of these particles is proof of the higher viscosity of their constituent phase during HIPing. Here too, EPMA analysis of the spheres confirmed a greater oxygen content in the grain boundary compared with the nitride matrix analysis. In both cases HIPing did not induce any change in the stoichiometry.

3.3. Thermomechanical properties

The Vickers microhardness follows classical law and increases when the porosity decreases (Fig. 3). Compared with the microhardness value of hard ZrN physical vapour deposited coatings [H_v (5 N) = 2600 kg mm^{-2}] [8], our value was much lower, but similar to those for sintered materials [9]. The difference in microhardness between the two grades was not significant. Tani *et al.* [10] observed no differences in the microhardness values of HIPed dense materials when the grain size varied from 0.2 to 214 μm. Therefore, the lightly higher value of the Cerac material observed should be related to the microstructure in a direct relationship with the presence of the oxynitride phase.

The statistical variation in strength (σ_f) at room temperature is shown as a function of porosity in Fig. 4. The maximum value was obtained for the first grade (σ_f = 335 MPa) with a standard deviation of 14. Observations by SEM of the fracture surfaces (Fig. 2b–d) did not really allow the fracture sources to be identified. In both materials the fractures were mixed inter- and intragranular. SEM observations of the Cerac grade demonstrated that, even if the porosity was high, the fractures always crossed the largest grains. On the other hand, the largest grains of the Starck grade were more resistant.

The fracture toughness values, in a similar way to the modulus of rupture values, depend on the porosity and increase regularly with increasing relative density (Fig. 5), but it is noted that the maximum porosity measured was about 8%.

The dependence of the powder properties on the modulus of rupture or the fracture toughness was perceptible but very slight. On the other hand, an important improvement was obtained by increasing the dwell time from 1 to 2 h. In both cases the increase in the modulus of rupture was close to 30 MPa and the toughness rise near 2 MPa m$^{1/2}$.

Knowing the modulus of rupture and fracture toughness, the largest defect size may be calculated using

$$a_c = K_{Ic}^2/1.21\pi\sigma_f^2 \quad (1)$$

The simplest inherent flaw observed was a pore. The pores were distributed uniformly throughout the bulk of the material and the large grains always contained a small amount of porosity. However, the calculated values of the defect size for dense material (81 and 125 μm) were much higher than the maximum pore size (< 1 μm). Obviously, in both cases the critical flaw size was much greater than the pore size. It could be associated with machining damage produced during the surface preparation process, but SEM observations showed an agglomeration of small particles which created a concentration of voids and induced a higher porosity. Near the surface this phenomenon may provoke rupture.

The empirical dependence of the elastic moduli on porosity has been widely discussed and many equations have been proposed to describe the elastic modulus–porosity relationship of oxides [11–13]. These equations were applied to our data and Table II gives the values of the Young's and shear moduli as well as the Poisson's ratio obtained by extrapolation of the data to zero porosity. The linear equation used

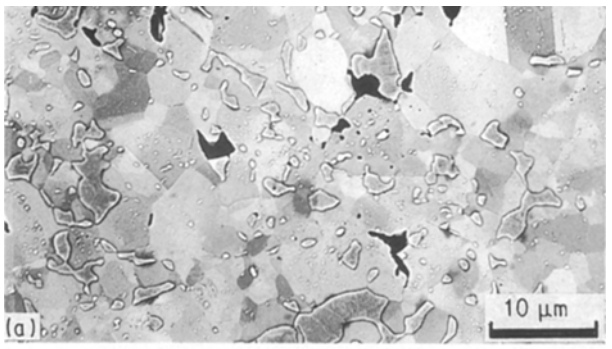

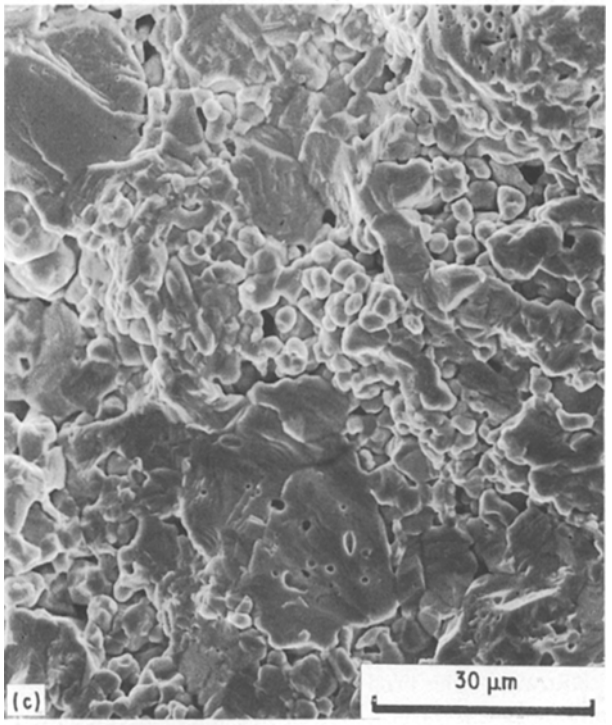

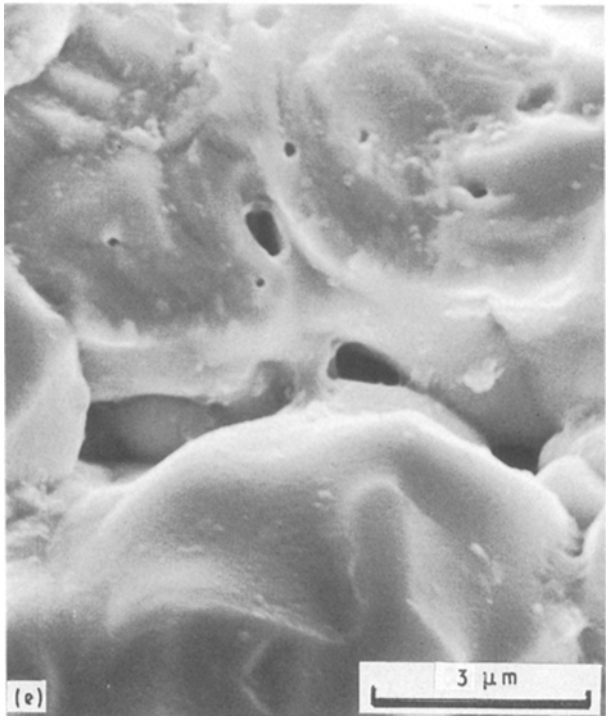

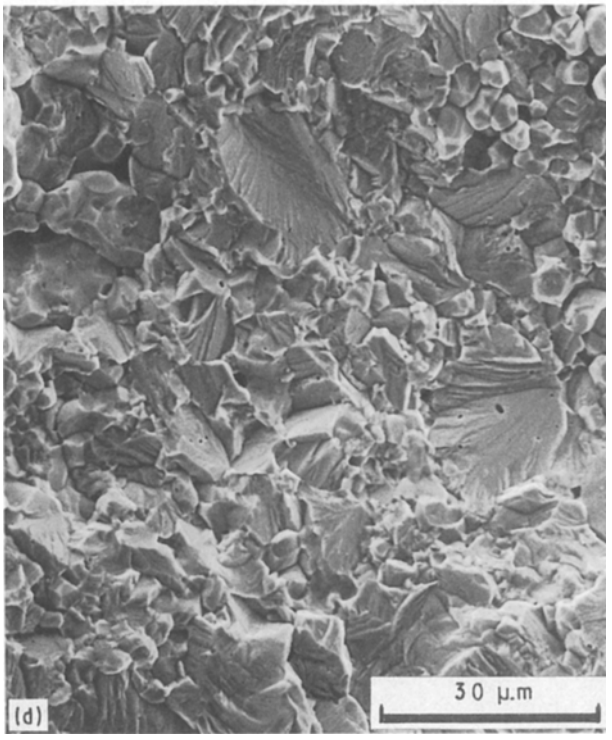

Figure 2 SEM micrographs of HIPed ZrN materials: (a) obtained by secondary electron emission (Cerac powder; 1600 °C, 190 MPa, 1 h), (b) fracture surface (Starck powder; 1600 °C, 195 MPa, 1 h), (c) fracture surface (porosity 8%, Cerac powder; 1600 °C, 120 MPa, 1 h), (d) fracture surface (Cerac powder; 1750 °C, 195 MPa, 1 h) and (e) bridging effect due to the viscosity of the oxynitride phase (porosity 6%, Cerac; 1550 °C, 1900 °C, 1 h).

is no longer valid at high porosity, but gives a good fit at low porosity (Fig. 6).

Comparing the two dense materials, no tangible difference in the elastic parameters was observed (Table III). In fact, our results confirm that elastic properties depend on the pore characteristics (size,

TABLE II Results of fitting data to different equations (Cerac grade)

	$M = M_0(1 - aP)$	$M = M_0[\exp(-aP)]$	$M = M_0\left(\frac{1-P}{1+aP}\right)$	$M = M_0(1 - aP^{2/3})$
E_0 (GPa)	388	389	389	409
G_0(GPa)	154	154	153.8	161.8
ν_0	0.259	0.259	0.260	0.262

TABLE III

Material	H_v(2 N)	f (MPa)	K_{Ic} (MPa $m^{1/2}$)	a_c (μm)	E (GPa)	G (GPa)	ν	γ (J m^{-2})
Cerac ■	1394 ± 90	335 ± 14	5.9 ± 0.5	81	382	153	0.256	42
Starck ☆	1273 ± 55	305 ± 28	6.6 ± 0.3	123	380	151	0.256	54

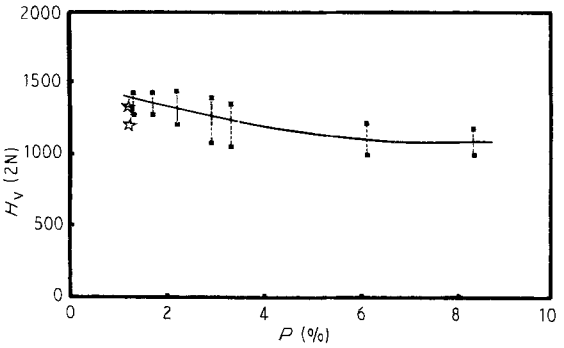

Figure 3 Evolution of Vickers microhardness with porosity.

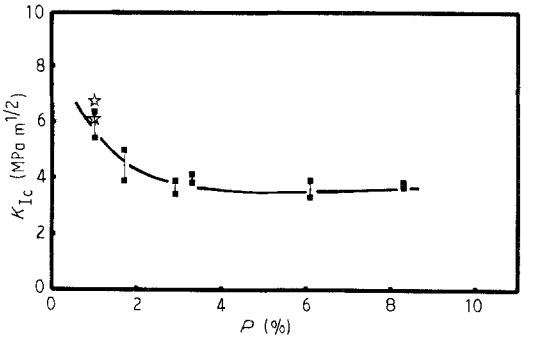

Figure 5 Influence of porosity on fracture toughness.

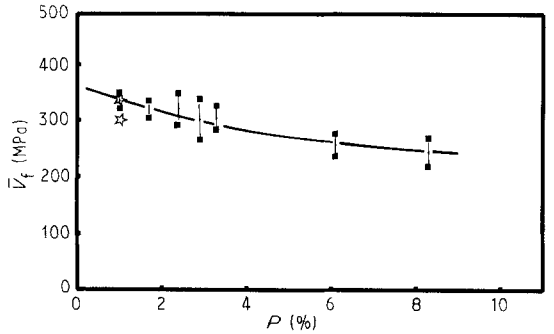

Figure 4 Evolution of fracture strength.

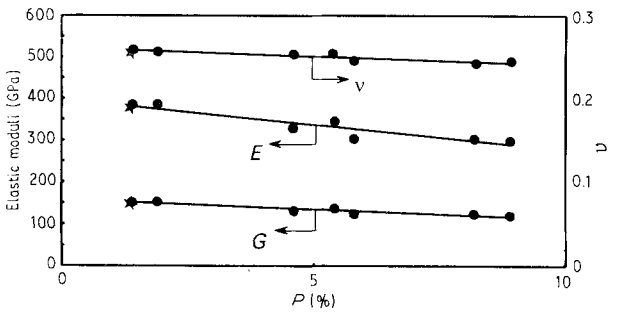

Figure 6 Elastic moduli and Poisson's ratio versus porosity curves.

location, shape, etc.) but not on the grain size. This last point has already been proved by Manning *et al.* [14] in a grain size field ranging from 1 to 200 μm.

Susceptibility to thermal shock is an important consideration in the use of these materials. Explanations and theory have been widely discussed by Hasselman [15].

In comparison with the dense transition-metal nitrides already studied (TiN $\Delta T_c = 210\,^{\circ}C$ [16] and TaN $\Delta T_c = 300\,^{\circ}C$) [17], the critical quenching temperature at which thermal shock damage first occurs corresponds to an intermediate value (Fig. 7). Moreover, the fine-grained material showed no significant improvement in the critical temperature difference ΔT_c and no damage was observed below 235 °C. Nevertheless, the shape of the thermal damage resistance curve changed with the nature of the material under load in relation to the microstructural parameters [18]. The strength evolution of thermally damaged Starck specimens occurred abruptly, the flaw size

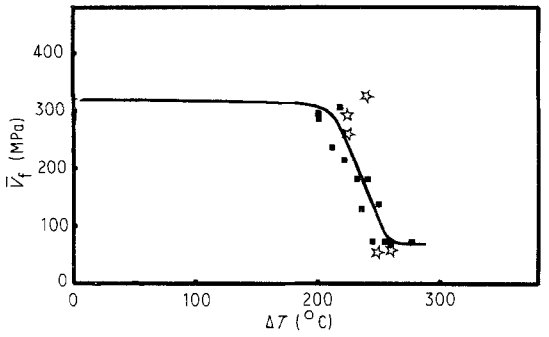

Figure 7 Thermal shock damage curve.

TABLE IV

Materials	Cerac	Starck
T_c (K)	235 ± 5	235 ± 5
R (K)	93	85
R'''' (μm)	192	296

mainly controlling the thermal shock resistance. On the other hand, the continuous transition in the resistance of the Cerac grade may be explained by the presence of a greater amount of oxynitride phase.

The thermal shock resistance was reduced by porosity effects. For the investigated Cerac material of 94% relative density, a value of 210 ± 5 °C was obtained. However, if only the porosity parameter changed, no effect on the shape of the curve was observed.

Two parameters of the thermal shock damage were analysed (Table IV) : the thermal stress transfer R (high Biot number 1) and the theoretical crack propagation resistance parameter R''''

$$R = \sigma_f(1 - \nu)/\alpha E \quad (2)$$

$$R'''' = \frac{E\gamma}{\sigma_f^2(1 - \nu)} = \frac{K_{Ic}^2(1 + \nu)}{2\sigma_f^2} \quad (3)$$

$$\gamma = (1 - \nu^2)K_{Ic}^2/2E \quad (4)$$

A value of $7 \times 10^{-6}\ K^{-1}$ was used for the coefficient of thermal expansion.

R is the maximum resistance to thermal cracking of the material. R'''' characterizes the minimum in the extent of crack propagation and gives quantitative information about the final crack length. An increase in the fourth thermal shock resistance parameter should correspond to an improvement of the material, because it corresponds to a decrease in the crack area.

The knowledge of these parameters allows a direct calculation of the effective surface energy by applying the general Equation 4. Ricę and Freiman [19] observed no significant dependence of the fracture energy on the grain size in the case of dense polycrystalline bodies. In our case the higher value for the second grade was directly related to the toughness (Table III).

4. Conclusion

In this work we investigated the sintering behaviour of two commercially available powders. In both cases a dense zirconium nitride material was obtained by HIPing.

The results clearly show that the densification behaviour is dependent on the characteristics of the starting powders. For a given temperature, an increased specific surface area leads to an enhancement in densification. On the other hand, an irregular shape and a large size distribution of particles induce severe sintering conditions, i.e. finer and more-spherical grains permit a dense material to be obtained at a lower temperature.

The thermal and mechanical properties of ceramics depend mainly on the porosity. At the same porosity, below 1%, the differences between the modulus of rupture and the critical stress intensity factor of the two grades were more tangible than between the elastic moduli or the thermal shock parameters. Despite the greater oxygen content in the first grade, the properties of the dense zirconium nitrides were very similar.

Acknowledgements

The technical assistance of B. Soulestin and L. Progeas was greatly appreciated. The authors express appreciation to Professor J. C. Glandus, whose contribution was valuable in performing elastic moduli measurements.

References

1. P. CHIOTTI, *J. Amer. Ceram. Soc.* **35** (1952) 123.
2. R. Y. PETRYKINA and L. K. SHVEDOVA, *Porosh. Metall.* **4**, 112, (1972) 27.
3. O. V. PSHENICHNAYA, M. A. KUZENKOVA and P. S. KISLYI, *ibid.* **12**, 156, (1975) 41.
4. O. A. JOHANSEN, J. H. DONTJE and R. L. D. ZENNER, *Thin Solid Films* **153** (1987) 75.
5. J. C. GLANDUS, T. ROUXEL and Q. TAI, *Ceram. Int.* **17** (1991) 129.
6. S. IKEDA, T. YAGI, N. ISHIZAWA, N. MIZUTANI and M. KATO, *J. Solid St. Chem.* **73** (1988) 52.
7. G. V. TENDELOO and G. THOMAS, *Acta Metall.* **10** (1983) 1611.
8. D. T. QUINTO, G. J. WOLFE and P. C. JINDAL, *Thin solid films* **153** (1987) 19.
9. G. V. SAMSONOV and V. S. NESHPOR, *Dokl. Akad. Nauk SSSR* **104** (1955) 405.
10. T. TANI, Y. MIYAMOTO, M. KOIZUMI and M. SHIMADA, *Ceram. Int.* **12** (1986) 33.
11. K. K. PHANI and S. NIYOGI, *J. Mater. Sci.* **22** (1987) 257.
12. *Idem, ibid.* **6** (1987) 511.
13. M. DESMAISON-BRUT, J. C. GLANDUS, J. MONTINTIN, F. VALIN and M. BONCOEUR, in Proceedings of the 7th CIMTEC, Montecatini, Italy, June 1990, edited by P. Vincenzini (Elsevier, Amsterdam, 1991) p. 1713.
14. W. R. MANNING, O. HUNTER and B. R. POWELL, *J. Amer. Ceram. Soc.* **52** (1969) 436.
15. D. P. H. HASSELMAN, *Amer. Ceram. Soc. Bull.* **49** (1970) 1033.
16. L. THEMELIN, M. DESMAISON-BRUT, M. BONCOEUR and F. VALIN, in Proceedings of the International Conference on HIP of Materials: Applications and Developments, Anvers, Belgium, April 1988, (The Royal Flemish Society of Engineers, 1988) p. 561.
17. J. MONTINTIN, M. DESMAISON-BRUT, M. BONCOEUR and F. VALIN in Proceedings of Hot Isostatic Pressing: Theory and Applications, Gaithersburg, Virginia, June 1989, edited by R. J. Schaefer and M. Linzer (American Society of Metals International, Materials Park, Ohio, 1991) p. 233.
18. G. ZIEGLER and J. HEINRICH, *Ceram. Int.* **6** (1980) 25.
19. R. W. RICE and S. W. FREIMAN, *J. Amer. Ceram. Soc.* **64** (1981) 350.

Received 2 January
and accepted 2 September 1992